SLAC-PUB-1647
September 1975
(T/E)

THE ψ RESONANCES AND SEARCHES FOR NEW PARTICLES*

G. J. Feldman

Stanford Linear Accelerator Center
Stanford University, Stanford, California 94305

INTRODUCTION

In the seven months since the discovery of the ψ particles we have been systematically studying their properties and decays at SPEAR. We have learned a great deal and most, but not all, of the pieces seem to be falling into place. I will review today the determination of the widths and quantum numbers of these particles and the ongoing study of their decay modes. I will also report on the total cross section for hadron production in e^+e^- annihilations and on searches for new particles.

THE MAGNETIC DETECTOR

The bulk of the data in this report come from the SLAC-LBL magnetic detector,[1,2] which is shown in Fig. 1. The detector has a solenoidal coil which

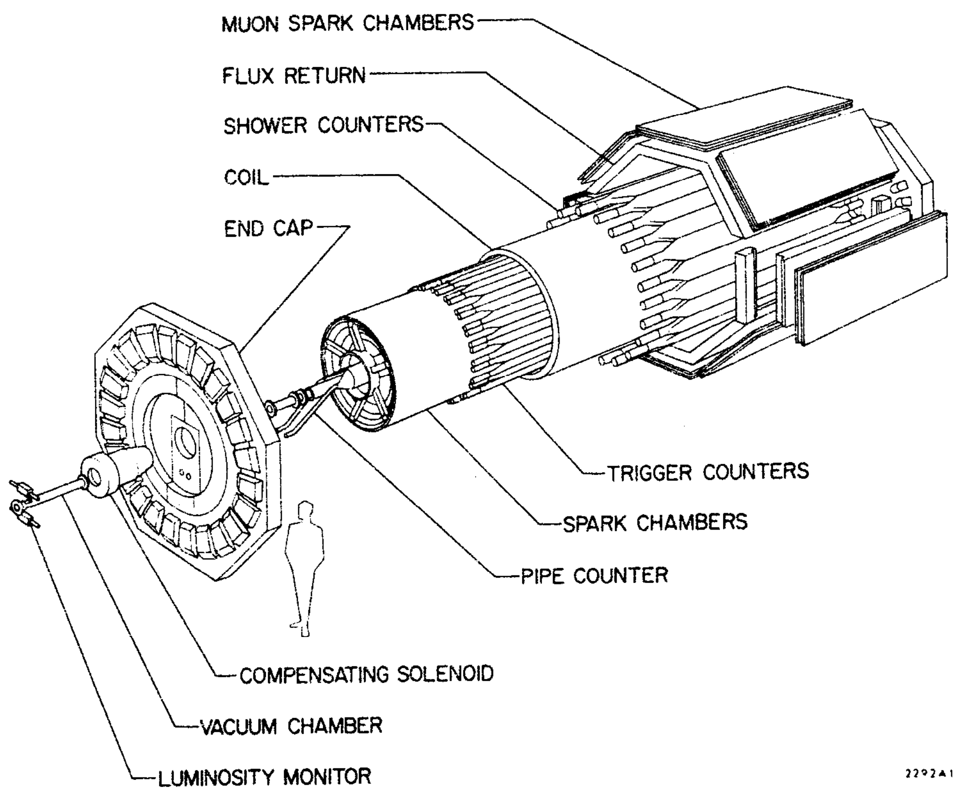

Fig. 1--Telescoped view of the SLAC-LBL magnetic detector.

* Work supported by the U.S. Energy Research and Development Administration and by a U.S. National Science Foundation International Travel Grant.
(Invited talk at the Fifth International Conference on Neutrino Science, Balatonfüred, Hungary, June 16-21, 1975.)

produces a magnetic field parallel to the incident beams. A set of cylindrical spark chambers measures trajectories of charged particles over about 70% of the full solid angle. Two cylindrical arrays of 48 trigger counters and 24 Pb-scintillator sandwich shower counters detect charged particles and γ-rays over about 65% of the solid angle. The trigger for an event is two or more charged particles which each fire a trigger and shower counter. Separation of π's, K's, and p's is accomplished by time-of-flight measurements in the trigger counters. π-K separation is possible up to momenta of about 700 MeV/c and K-p separation is possible to momenta of about 1 GeV/c. Electrons can be identified as particles which cause large pulse heights in the shower counters and muons can be identified as particles which penetrate the flux return and fire the muon spark chambers.

I will also report one result from a Stanford experiment which was situated in the other interaction region of SPEAR. Figure 2 shows the apparatus. The main purpose of the experiment was to study quantum electrodynamics. However, the large NaI crystals were also useful to search for monochromatic photons from ψ' decay.

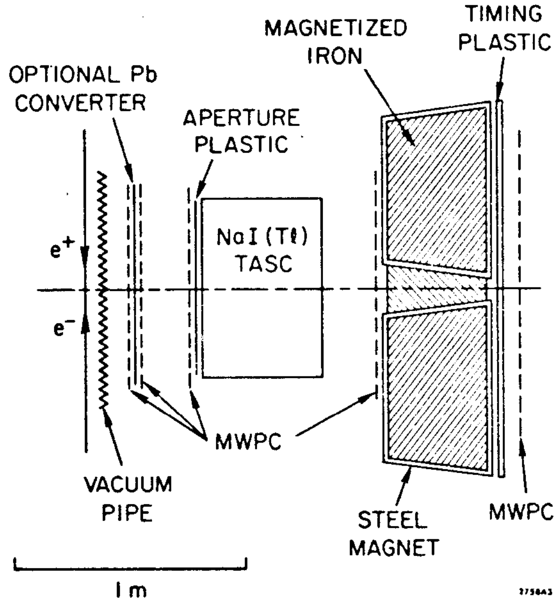

Fig. 2--One of the two NaI crystal spectrometers of the Stanford experiment.

WIDTHS OF THE ψ AND ψ'

Figures 3 and 4 show the apparent cross sections for hadron production, μ pair production, and e pair production (or scattering) in the vicinity of the ψ and ψ'.[3,4] These are only apparent cross sections because in both cases the widths of the resonances are considerably smaller than the experimental resolution.

To obtain apparatus-independent values for the cross sections we integrate over energy to obtain

$$\Sigma_{\psi} = \int \sigma_{\psi}(E)dE = 10400 \pm 1500 \text{ nb} \cdot \text{MeV} \tag{1}$$

$$\Sigma_{\psi'} = \int \sigma_{\psi'}(E)dE = 3700 \pm 600 \text{ nb} \cdot \text{MeV} . \tag{2}$$

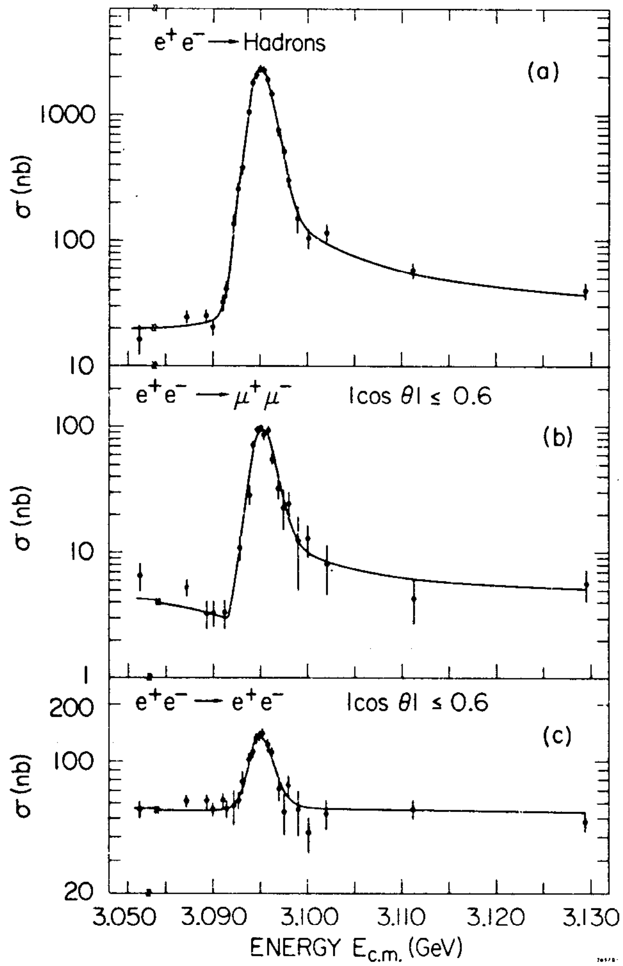

Fig. 3--Cross sections in the region of the ψ. The curves are fits to all the data, including interference and radiative effects.

These integrated cross sections are corrected for the rather considerable effect of initial state radiation.[5]

The measurement of the leptonic and hadronic cross sections together allows us to calculate the true ψ widths in a simple way. For any state f, the resonant cross section will be given by

$$\sigma_{\psi,f} = \frac{\pi(2J+1)}{m^2} \frac{\Gamma_{ee}\Gamma_f}{(E-m)^2 + \Gamma^2/4} , \tag{3}$$

where m is the mass of the ψ, J is its spin, Γ_f is the partial decay width to the state f, and Γ is the total decay width.

Integrating Eq. (3) and using J = 1 (which we will establish in a few minutes), we obtain

$$\Sigma_{\psi,f} = \int \sigma_{\psi,f}\, dE = \frac{6\pi^2}{m^2} \frac{\Gamma_{ee}\Gamma_f}{\Gamma} . \tag{4}$$

We can now use Eq. (4) to obtain all of the widths. In particular,

$$\boxed{\Gamma_{ee} = \frac{m^2}{6\pi^2} \Sigma_{\psi,all}} \tag{5}$$

and

$$\Gamma = \frac{\Sigma_{\psi,all}}{\Sigma_{\psi,ee}} \Gamma_{ee} . \tag{6}$$

For simplicity we have ignored radiative effects and interference between ψ decays and the direct channel $e^+e^- \to f$. These effects can be included in a straightforward way. When this is done we obtain the results given in Table I.

The astonishingly small widths of the ψ particles, about 70 keV and 200 keV, are, of course, what make these particles so remarkable.

QUANTUM NUMBERS OF THE ψ AND ψ'

Since the ψ particles are produced in e^+e^- annihilation, our first guess is that, like the vector mesons, they couple directly to the photon and thus have the same quantum numbers, $J^{PC} = 1^{--}$. This would not have to be the case, however, if they coupled directly to leptons.

We can determine the quantum numbers directly by observing the interference between the leptonic decays of the ψ particles,

$$e^+e^- \rightarrow \psi \rightarrow e^+e^- \quad (7)$$

and

$$e^+e^- \rightarrow \psi \rightarrow \mu^+\mu^- \quad (8)$$

and the direct production of lepton pairs,

$$e^+e^- \rightarrow e^+e^- \quad (9)$$

and

$$e^+e^- \rightarrow \mu^+\mu^- \quad . \quad (10)$$

The amplitude for reaction (10) is

$$A(e^+e^- \rightarrow \mu^+\mu^-) = \left(\frac{3\pi}{E^2}\right)^{\frac{1}{2}} \left(-\frac{2\alpha}{3}\right), \quad (11)$$

and the amplitude for reaction (8) is

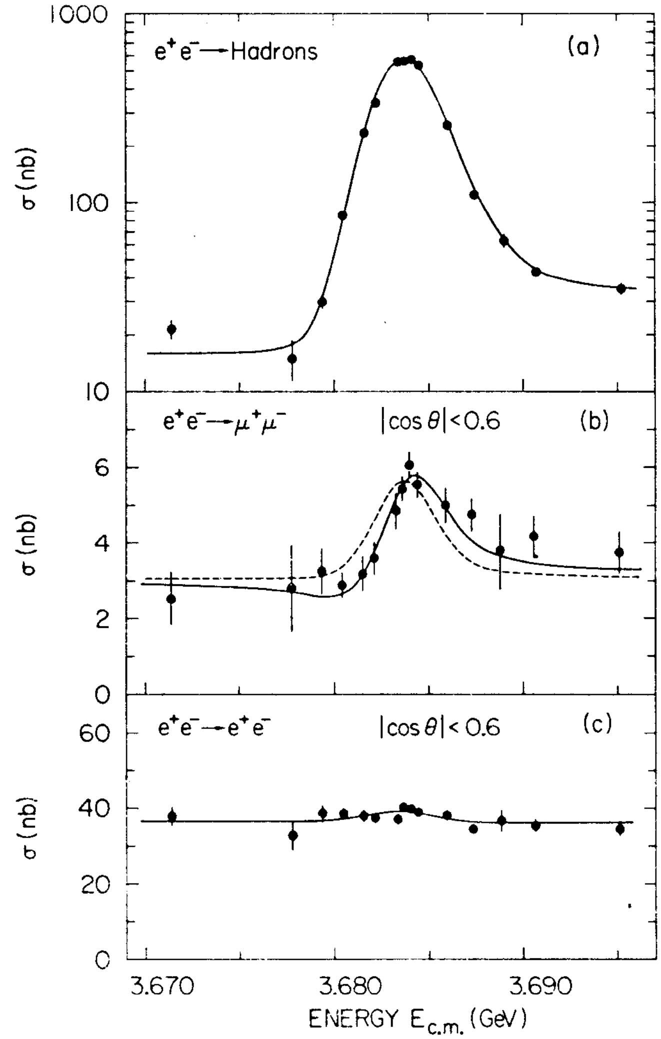

Fig. 4--Cross sections in the region of the ψ'. The curves are fits to all the data, including interference and radiative effects.

TABLE I

Widths of the ψ particles. Γ_h is the partial width to hadronic final states.

	ψ	ψ'
Γ_{ee}	4.8 ± 0.6 keV	2.2 ± 0.3 keV
$\Gamma_{\mu\mu}$	4.8 ± 0.6 keV	$\Gamma_{ee} = \Gamma_{\mu\mu}$ assumed
Γ_h	59 ± 14 keV	220 ± 56 keV
Γ	69 ± 15 keV	225 ± 56 keV
Γ_{ee}/Γ	0.069 ± 0.009	0.0097 ± 0.0016
Γ_h/Γ	0.86 ± 0.02	0.981 ± 0.003
$\Gamma_{\mu\mu}/\Gamma_{ee}$	1.00 ± 0.05	0.89 ± 0.16

$$A(e^+e^- \to \psi \to \mu^+\mu^-) = \left(\frac{(2J+1)\pi}{E^2}\right)^{\frac{1}{2}} \frac{\Gamma_{ee}}{m-E-i\Gamma/2} \qquad (12)$$

If the ψ particles have the quantum numbers of the photon, the cross section will have the form

$$\frac{d\sigma}{d\theta} = \frac{9\pi}{8\,E^2}\,(1+\cos^2\theta)\left|-\frac{2\alpha}{3} + \frac{\Gamma_{ee}}{m-E-i\Gamma/2}\right|^2 \qquad (13)$$

The sum of the amplitudes which go into Eq. (13) is shown graphically in Fig. 5. As the resonance proceeds around the diagram, it is clear that there will be destructive interference below the resonant energy. The ratio of muon pairs to electron pairs as a function of energy is shown for the ψ and the ψ' in Fig. 6. This ratio is used because it is least sensitive to normalization effects and because the electron pairs are expected to have a small constructive interference below the resonance (due to interference with the spacelike diagram).

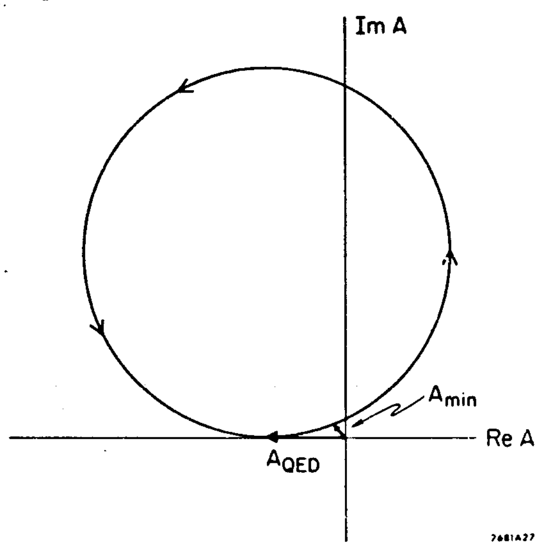

Fig. 5--Schematic drawing of the amplitude for production of μ pairs in the ψ region assuming that the ψ has the same quantum numbers as the photon. A_{QED} is the amplitude for direct production of μ pairs far below and far above the resonant energy. A_{min} is the amplitude at the point of maximum destructive interference below the resonant energy.

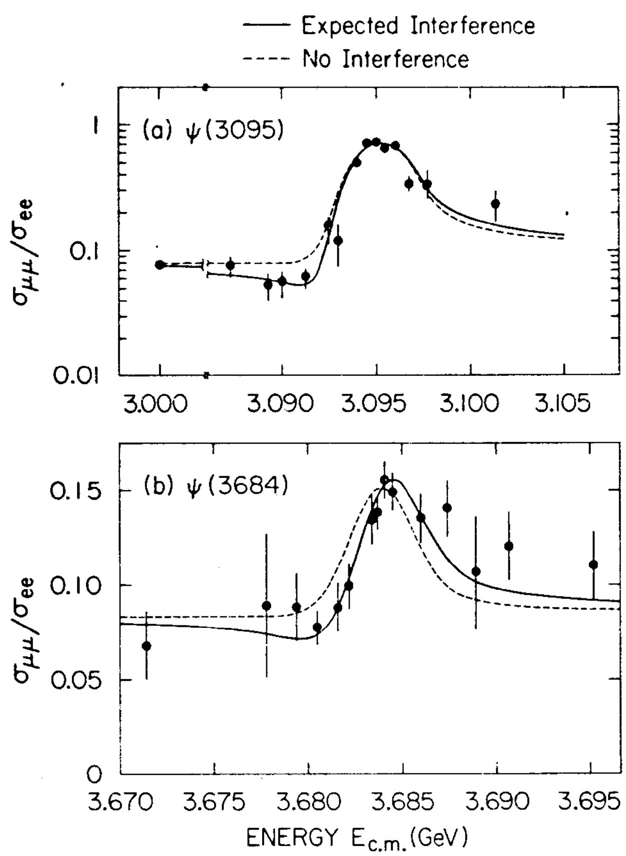

Fig. 6--The ratio of μ pair yield to e pair yield in the region of the ψ particles for $|\cos\theta| \leq .6$. The dashed line gives the expected ratio for no interference while the solid line gives the expected ratio for full interference. Radiative and resolution effects are included.

The data are inconsistent with no interference by 2.7 standard deviations in the ψ region and by 4.9 standard deviations in the ψ' region. This is sufficient to confirm our first guess, that the quantum numbers of both the ψ and ψ' are those of the photon, $J^{PC} = 1^{--}$.

Figure 7 shows the front-back μ pair charge asymmetry measured as a function of energy. The lack of any large asymmetry confirms the P and C assignments and argues against the possibility of the ψ particles not being eigenstates of P or C or of being degenerate with other nearby states having even P or C.

G PARITY AND ISOSPIN OF THE ψ

We can determine the G parity of the ψ by observing whether it decays into even or odd numbers of pions. It turns out that the ψ decays into both even and odd numbers of pions - a violation of I spin. However, this violation occurs in precisely the way we expect it to occur, and in the way it is required to occur, if the ψ couples to a photon.

Consider the three diagrams in Fig. 8. Figure 8(a) shows the direct decay of the ψ into hadrons, (b) shows the decay of the ψ into hadrons via an intermediate photon, and (c) shows the decay into μ pairs. In

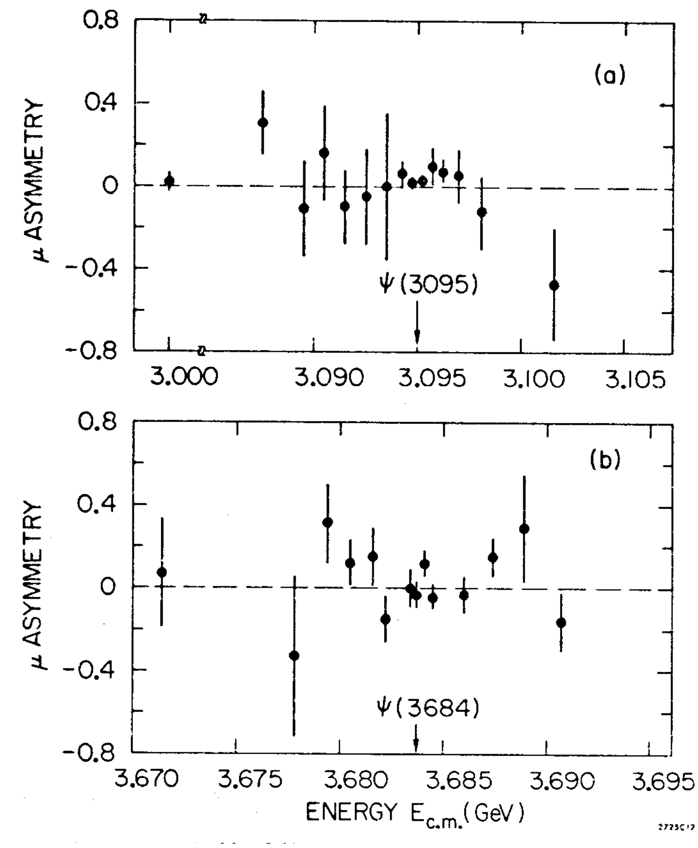

Fig. 7--The front-back asymmetry for μ pair production in the region of the ψ particles. The asymmetry is defined as the number of positive muons produced in the direction of the incident positron minus the number of negative muons produced in the direction of the incident positron all divided by the number of muon pairs.

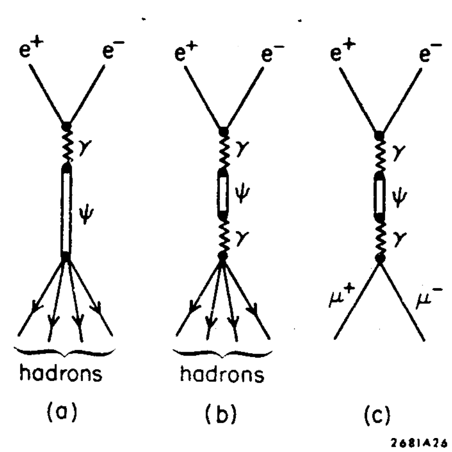

Fig. 8--Feynman diagrams for
(a) the direct ψ decay to hadrons
(b) the ψ decay to hadrons via an intermediate photon
(c) the ψ decay to μ pairs.

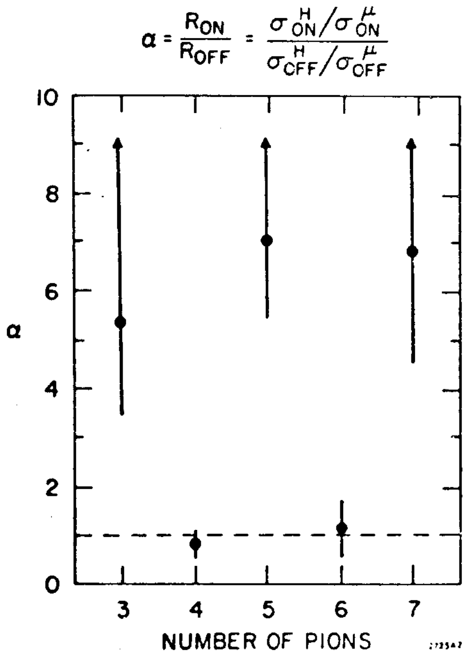

Fig. 9--Comparison of the ratio of pion production to $\mu^+\mu^-$ production on and off the ψ resonance.

(b), the nature of the final state, except for a phase factor, must be the same as the non-resonant final state produced in e^+e^- annihilation at the same energy. This state need not conserve isospin and may be quite different from the state produced by (a). Furthermore, we know what contribution (b) must make because the ratio between (b) and (c) must be the same as it would be if the ψ were not in the diagram, about 2.5. Thus, from the data in Table I, we deduce that if the ψ couples to a photon (a) contributes 68% to the width of the ψ, (b) contributes 18%, and the leptonic modes contribute 14%.

To test this hypothesis we want to compare the ratio of all pion state cross sections to μ pair cross section on and off-resonance. We compute the ratio α, defined

$$\alpha = \frac{\sigma^{\psi}_{n\pi}}{\sigma^{\psi}_{\mu\mu}} \bigg/ \frac{\sigma^{3.0}_{n\pi}}{\sigma^{3.0}_{\mu\mu}} , \tag{14}$$

where data at 3.0 GeV are used as the off-resonance sample. Values of α for three to seven pion production are shown in Fig. 9. The results are consistent with all of the even number of pion production (G even, I odd) coming from the intermediate photon decay, Fig. 8b. Most of the odd pion production comes from the direct ψ decay, Fig. 8a, and the ψ appears to decay directly into a pure $I^G = (\text{even})^-$ state.

It is relatively easy to show that I=0. Figure 10 shows the Dalitz plot for $\psi \rightarrow 3\pi$. This channel is clearly dominated by $\psi \rightarrow \rho\pi$, which implies that either $I = 0$ or $I = 2$. If $I = 0$, then $\Gamma_{\rho^0\pi^0} = \Gamma_{\rho^+\pi^-}$, whereas for $I = 2$, $\Gamma_{\rho^0\pi^0} = 4\Gamma_{\rho^+\pi^-}$. The

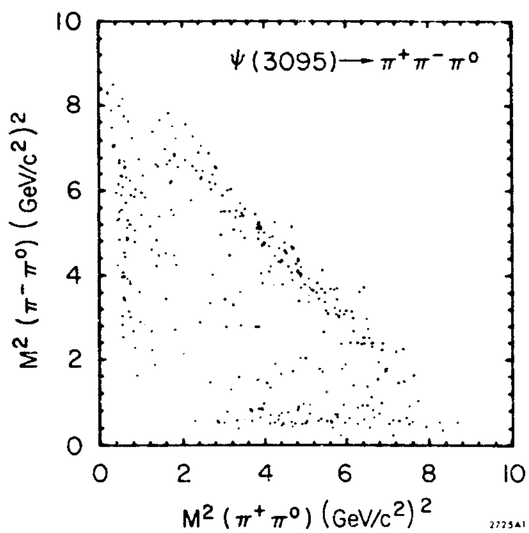

Fig. 10--Dalitz plot for the decay $\psi \rightarrow \pi^+\pi^-\pi^0$. The data are not corrected for experimental biases.

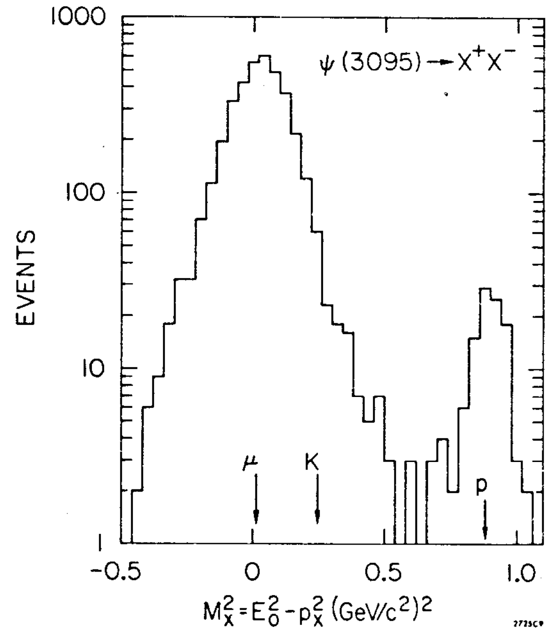

Fig. 11--Mass squared for collinear 2-prong events excluding electron pairs.

data indicate that $\Gamma_{\rho^0\pi^0} = (1.18 \pm 0.34)\ \Gamma_{\rho^+\pi^-}$, strongly favoring I = 0.

Another, and somewhat more direct, argument for I = 0 is found in the observation of the decay $\psi \rightarrow p\bar{p}$. This decay is separated from $\psi \rightarrow \mu^+\mu^-$ by kinematics, as demonstrated in Fig. 11. A comparison with 3.0 GeV data, in which no $p\bar{p}$ events were observed, indicates that this is a direct decay. A $p\bar{p}$ state has either I = 0 or I = 1 and, since I is even, only I = 0 is allowed in this case.

OTHER HADRONIC DECAYS AND THE SU(3) CHARACTER OF THE ψ

Table II is a list of branching ratios or limits for various decay modes of the ψ which have been identified or searched for in the SLAC-LBL magnetic detector. The study of hadronic decays is just beginning and promises to provide a great deal of interesting information.

For example, we can make some observations on the possible SU(3) classification of the ψ by examining Table II. If we look at the quasi-two-body decays involving kaons, we note that all of the modes which are forbidden for an SU(3) singlet, $K_S^0K_L^0$, $K^0\bar{K}^{0*}(1420)$, $K^\pm$, $K^{\mp*}(1420)$, $K^{0*}(892)\bar{K}^{0*}(892)$, and $K^{0*}(1420)\bar{K}^{0*}(1420)$ have not been observed. However, other modes which are allowed for an SU(3) singlet, $K^0\bar{K}^{0*}(892)$, $K^\pm K^{\mp*}(892)$, and $K^{0*}(892)\bar{K}^{0*}(1420)$, have been identified. These measurements are an indication that the ψ may be an SU(3) singlet. However, SU(3) cannot be exact for this would require

$$\frac{1}{3}\Gamma_{\rho\pi} = \frac{1}{4}\left(\Gamma_{K^0K^{0*}} + \Gamma_{K^\pm K^{\mp*}}\right) . \tag{15}$$

This relationship is violated by a factor of 2 to 3, even after correcting for phase space differences.

$\psi' \rightarrow \psi$ DECAYS

The ψ' decays over half the time into the ψ, primarily via the decay mode

$$\psi' \rightarrow \psi\pi\pi . \tag{16}$$

TABLE II

Decay Modes of the $\psi(3095)$

Mode	Branching Ratio (%)	No. of Events Observed	Comments
e^+e^-	6.9 ± 0.9	ca 2000	
$\mu^+\mu^-$	6.9 ± 0.9	ca 2000	
$\rho\pi$	1.3 ± 0.3	153 ± 13	$>70\%$ of $\pi^+\pi^-\pi^0$
$2\pi^+ 2\pi^-$	0.4 ± 0.1	76 ± 9	
$2\pi^+ 2\pi^- \pi^0$	4.0 ± 1.0	675 ± 40	$\left\{\begin{array}{l}20\%\ \omega\pi^+\pi^- \\ 30\%\ \rho\pi\pi\pi\end{array}\right.$
$3\pi^+ 3\pi^-$	0.4 ± 0.2	32 ± 7	
$3\pi^+ 3\pi^- \pi^0$	2.9 ± 0.7	181 ± 26	
$4\pi^+ 4\pi^- \pi^0$	0.9 ± 0.3	13 ± 4	
$\pi^+\pi^- K^+K^-$	0.4 ± 0.2	83 ± 18	$\left\{\begin{array}{l}\text{not including} \\ K^*(892)\ K^*(1420)\end{array}\right.$
$2\pi^+ 2\pi^- K^+K^-$	0.3 ± 0.1		
$K_S K_L$	<0.02	≤ 1	90% C.L.
$K^0 K^{0*}(892)$	0.24 ± 0.05	57 ± 12	
$K^\pm K^{\mp *}(892)$	0.31 ± 0.07	87 ± 19	
$K^0 K^{0*}(1420)$	<0.19	≤ 3	90% C.L.
$K^\pm K^{\mp *}(1420)$	<0.19	≤ 3	90% C.L.
$K^{*0}(892)\bar{K}^{*0}(892)$	<0.06	≤ 3	90% C.L.
$K^{*0}(1420)\bar{K}^{*0}(1420)$	<0.18	≤ 3	90% C.L.
$K^{*0}(892)K^{*0}(1420)$	0.37 ± 0.10	30 ± 7	
$p\bar{p}$	0.21 ± 0.04	105 ± 11	$\left\{\begin{array}{l}\text{assuming} \\ f(\theta) \sim 1+\cos^2\theta\end{array}\right.$
$\Lambda\bar{\Lambda}$	0.16 ± 0.08	19 ± 5	
$\left.\begin{array}{l} p\bar{p}\ \pi^0 \\ \bar{n}p\pi^- \\ \bar{p}n\pi^+ \end{array}\right\}$	0.37 ± 0.19	87 ± 30	

These decays are visible in the data in two major ways.[6] Figure 12 shows the missing mass recoiling against all combinations of $\pi^+\pi^-$. The ψ is clearly visible and the branching ratio

$$\frac{\psi' \to \psi\pi^+\pi^-}{\psi \to \text{all}} = 0.32 \pm 0.04 \tag{17}$$

can be determined from it.

Alternatively one can search for inclusive ψ decays by looking for the leptonic decay of the ψ in the ψ' data. Figure 13 shows the invariant mass distribution of the two highest momentum oppositely charged particles in each ψ' decay. (The particles are assumed to be muons, and electrons have been eliminated.) There are two well separated peaks, one around 3.7 GeV corresponding to ψ' decays to μ pairs plus the direct production of μ pairs and one around 3.1 GeV from

$$\psi' \to \psi + \text{anything} \; . \qquad \psi \to \mu^+\mu^- \tag{18}$$

These data yield

$$\frac{\psi' \to \psi + \text{anything}}{\psi' \to \text{all}} = 0.57 \pm 0.08 \; . \tag{19}$$

From Eqs. (17) and (19) we discover that

$$\frac{\psi' \to \psi\pi^+\pi^-}{\psi' \to \psi + \text{anything}} = 0.56 \pm 0.03 \; . \tag{20}$$

(The error in Eq. (20) is smaller than the combined errors of Eqs. (18) and (19) because of correlations in the errors.)

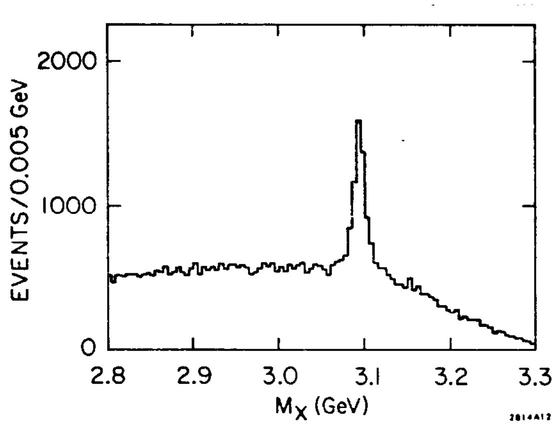

Fig. 12--The distribution of missing mass recoiling against all pairs of oppositely charged particles at the ψ'.

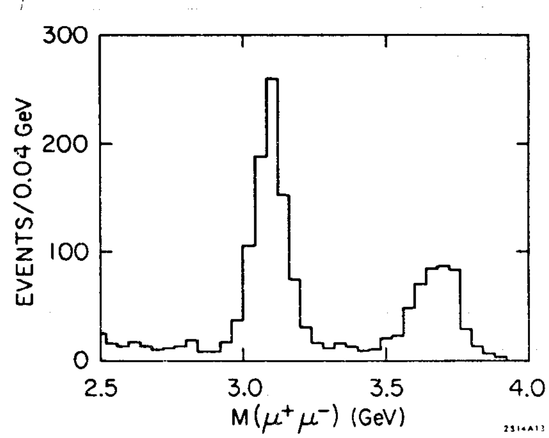

Fig. 13--The distribution of the $\mu^+\mu^-$ invariant mass for the highest momentum oppositely charged particle pair from each ψ' event. Electron pairs are excluded.

Since the ψ' decays via

$$\psi' \to \psi\pi^+\pi^- \qquad (21)$$

we also expect

$$\psi' \to \psi\pi^0\pi^0 \quad . \qquad (22)$$

If these are the only modes for $\psi' \to \psi$ decays and the ψ' is in a definite state of isospin then we expect Eq. (20) to have the values

$$\frac{\psi' \to \psi\pi^+\pi^-}{\psi' \to \psi + \text{anything}} = \begin{matrix} 0.66 \text{ for } I = 0 \\ 1.00 \text{ for } I = 1 \\ 0.32 \text{ for } I = 2 \end{matrix} \quad . \qquad (23)$$

(The Clebsch-Gordan coefficients have been corrected for phase space.) Clearly I = 0 is preferred.

If we assume that the ψ', like the ψ, decays to a pure isoscalar state, the difference between Eqs. (23) and (20) indicates that there are other $\psi' \to \psi$ modes with branching ratios

$$\frac{\psi' \to \psi + \text{neutrals (not } \pi^0\pi^0)}{\psi' \to \text{all}} =$$

$$= 0.09 \pm 0.03 \quad . \qquad (24)$$

To investigate these modes we subtract 3/2 of the $\psi' \to \psi\pi^+\pi^-$ spectrum from the $\psi' \to \psi$ + anything spectrum and plot the result in Fig. 14. The peak around a mass squared of 0.3 $(\text{GeV}/c^2)^2$ is evidence for the mode $\psi' \to \psi\eta$ which is observed in both the charged and neutral decay mode with a branching ratio

$$\frac{\psi' \to \psi\eta}{\psi' \to \text{all}} = 0.04 \pm 0.02 \quad . \qquad (25)$$

We don't know directly what the remaining events in Fig. 14 are. However there are two pieces of circumstantial evidence that they are the mode $\psi' \to \psi\gamma\gamma$:

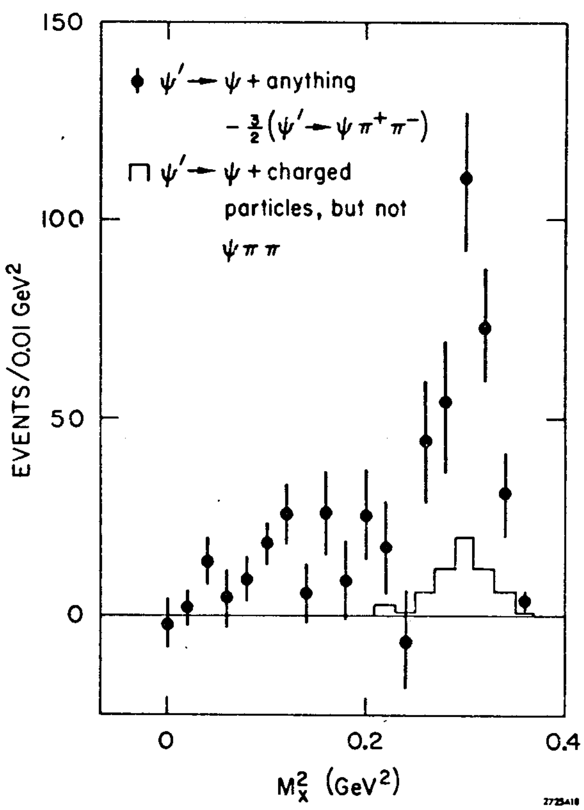

Fig. 14--The missing mass squared to the ψ corresponding to $\psi' \to \psi$ + anything - $3/2(\psi' \to \psi\pi^+\pi^-)$. The solid line indicates the missing mass squared spectrum of events in which the ψ and an additional charged particle are detected, but the detected particles are not kinematically compatible with $\psi' \to \psi\pi^+\pi^-$.

i) This is the only mode left with reasonable quantum numbers.

ii) There are events below the $2\pi^0$ threshold at the 2.3 standard deviation level.

There is no evidence at present that the $\gamma\gamma$ mode goes via an intermediate state; it could be a direct electromagnetic decay. If it does go by an intermediate state, then from the allowed kinematics[7] we can set an upper limit of

$$\frac{\psi' \to \psi\gamma\gamma}{\psi' \to \text{all}} < 0.066 \text{ at the 90\% confidence level.} \tag{26}$$

We are presently studying these $\gamma\gamma$ mode candidate events for evidence of intermediate states. (See the postscript to this report for post-conference developments.)

SEARCH FOR MONOCHROMATIC PHOTONS IN ψ' DECAYS

Another, and more general, method of searching for intermediate states is to look for the monochromatic photons directly. Two such searches have been done, one in the SLAC-LBL magnetic detector and the other in the Stanford experiment. Neither has found significant evidence for such photons.

The motivation for these searches was that if the ψ and ψ' are bound states of charm quarks, then other bound states should exist which the ψ' could decay into by the emission of a photon.[8] Some of these states could then decay into $\psi\gamma$, giving the sequence $\psi' \to \psi\gamma\gamma$. The most likely transitions in this scheme are shown in Fig. 15.

In the magnetic detector, the search was conducted by looking for photon conversions in the 0.052 radiation lengths of material which surround the interaction region. The observed momentum spectrum is shown in Fig. 16. The solid line represents the shape of the expected background from π^0 decay. The present analysis does not detect charged particles with momenta below 80 MeV/c and this accounts for the dropoff between 300 and 160 MeV.

In the Stanford experiment[9] the photon energies were measured in large NaI crystals. Data are presented separately in Fig. 17 for photons which convert in lead converters in front of the crystals and for those which fail to convert. In the latter case the trigger requirements are more restrictive.

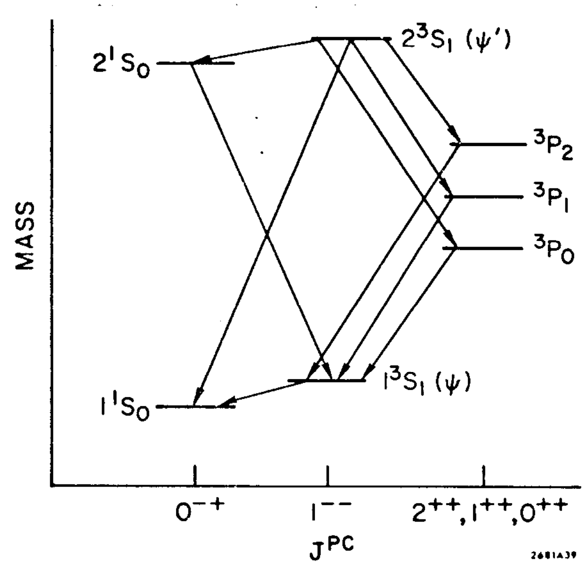

Fig. 15--The most likely gamma ray transitions in the charm model.

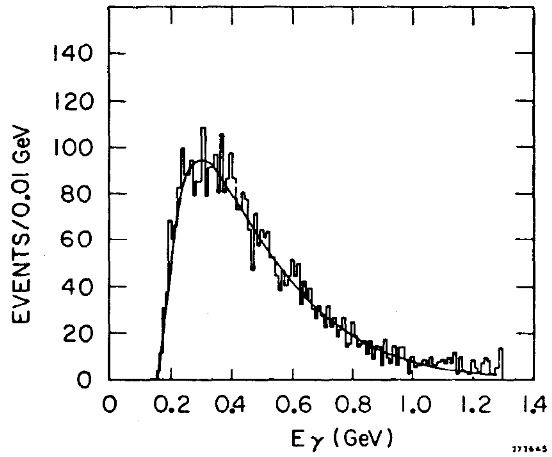

Fig. 16--Observed energy spectrum of converted photons in ψ' decays observed by the SLAC-LBL experiment. The solid line exhibits the shape of spectrum expected from π^0 decay.

The momentum resolution and upper limits on the branching ratio B,

$$B = \frac{\psi' \to \gamma X}{\psi' \to \mathrm{all}} \tag{27}$$

where X is a narrow state, are given in Table III for both experiments.

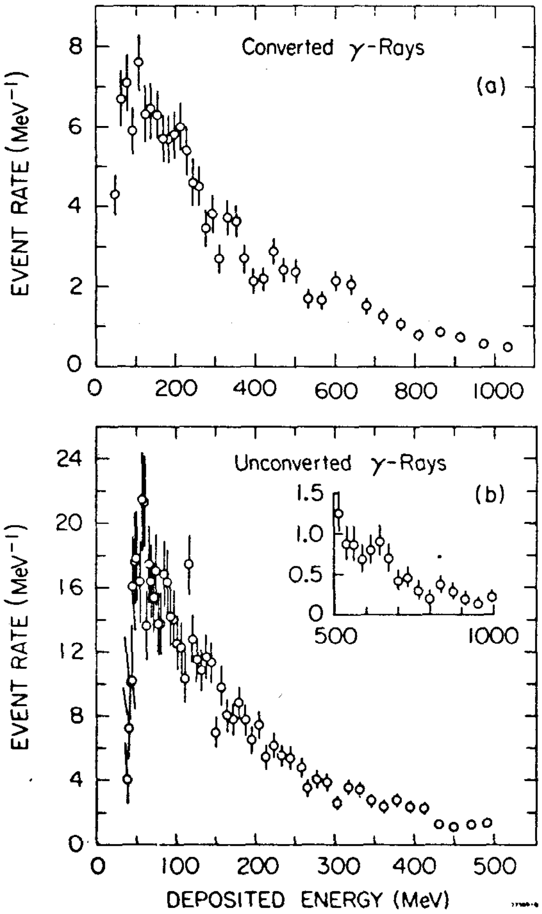

Fig. 17--Observed energy spectrum of (a) converted and (b) unconverted photons in ψ' decays observed by the Stanford experiment.

TABLE III
Limits on Monochromatic Radiative ψ' Decays

γ-ray Energy (GeV)	SLAC-LBL		Stanford			
			Converted γ's		Unconverted γ's	
	$\frac{dp}{p}$ (a)	B (b)	$\frac{dp}{p}$ (a)	B (c)	$\frac{dp}{p}$ (a)	B (c)
0.075	-	-	.075	.05	.019	.06
0.15	-	-	.047	.04	.019	.09
0.25	.03	.05	.033	.04	.019	.08
0.40	.03	.03	.025	.01	.019	.06
0.60	.03	.02	.025	.05	.019	.04
0.80	.03	.02	.025	.005	.019	.015

(a) rms resolution.

(b) Upper limit on the branching ratio at 90% confidence level.

(c) Upper limit on the branching ratio at 99% confidence level.

OTHER ψ' DECAYS

Table IV contains a summary of the known ψ' decays. No decays to ordinary hadrons have been identified in sharp contrast to the decays of the ψ (see Table II). The difference between ψ and ψ' decays is shown graphically in Fig. 18. Fig. 18a is a

TABLE IV
Decay Modes of the $\psi(3684)$

Mode	Branching Ratio (%)	Comments
e^+e^-	0.97 ± 0.16	μ-e universality assumed
$\mu^+\mu^-$	0.97 ± 0.16	
$\psi(3095)$ anything	57 ± 8	
$\psi(3095)\ \pi^+\pi^-$	32 ± 4	these decays are included in the fraction for ψ + anything
$\psi(3095)\ \eta$	4 ± 2	
$\psi(3095)\ \gamma\gamma$	< 6.6*	via an intermediate state
$\rho^0\pi^0$	< 0.1*	
$2\pi^+ 2\pi^- \pi^0$	< 0.7*	
$p\bar{p}$	< 0.03*	

* 90% confidence limit based on a preliminary analysis

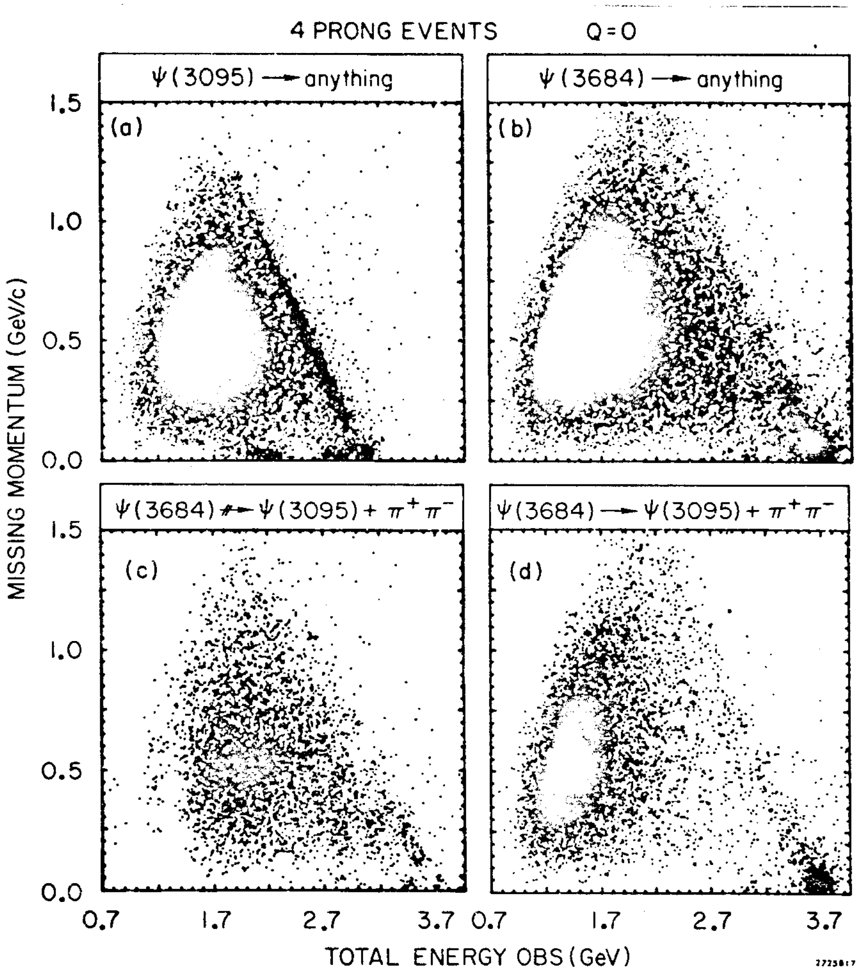

Fig. 18--Scatter plots of missing momentum versus total observed energy of four-prong events assuming that all tracks are pions. (a) All 4-prong events at ψ; (b) all 4-prong events at ψ'; (c) 4-prong $\psi' \to \psi\pi^+\pi^-$ events; (d) events in (b) with events from (c) removed.

scatter plot of the missing momentum versus the total observed energy (assuming all observed particles are pions) for four-prong events in ψ decays. Dense areas near missing momentum of zero correspond to $\psi \rightarrow 4\pi^{\pm}$, $\psi \rightarrow \pi^{+}\pi^{-}K^{+}K^{-}$, and $\psi \rightarrow \pi^{+}\pi^{-}p\bar{p}$. The dense diagonal band corresponds to $\psi \rightarrow 4\pi^{\pm}\pi^{0}$. Fig. 18b shows the same plot for the ψ', Fig. 18c shows the contribution of $\psi' \rightarrow \pi^{+}\pi^{-}$ to Fig. 18b, and finally Fig. 18d shows the difference between Figs. 18b and 18c, that is, ψ' decays with $\psi' \rightarrow \psi\pi^{+}\pi^{-}$ removed. The structures that were evident in Fig. 18a are not evident in Fig. 18d.

By adding up the $\psi' \rightarrow \psi$ decays, the leptonic decays, and the second order electromagnetic decays, we can account for 62 ± 8% of ψ' decays. The remaining 38 ± 8% of the decays are somewhat of a mystery.

(See the postscript for a possible start to the unraveling of this mystery.)

TOTAL HADRONIC CROSS SECTION

So far we have been discussing regions which comprise only 5 MeV in center-of-mass energy. We have, however, made measurements over 5 GeV and these are also of interest.

Figure 19a shows the total hadronic cross section as a function of center-of-mass energy and Fig. 19b shows the ratio R of the total cross section to the μ pair production cross section. The data through 5 GeV have been published[10] while the data from 5.6 GeV through 7.4 GeV are new preliminary results. The positions of the ψ and ψ' are indicated by arrows. On the scale of this plot, they are infinitesimally narrow spikes.

There are two regions where R appears to be constant - below 3.5 GeV where $R \approx 2.5$ and above 4.8 GeV where $R \approx 5.5$. There is an enhancement around 4.1 GeV which is probably a resonance, but might possibly be a threshold enhancement. We presently have little experimental information about this region, but we are currently acquiring more data.

In a quark-parton model R is just the sum of the squares of the quarks. Thus the two plateaus in R suggest that new quarks are being coupled to at the higher energies and that, correspondingly, new particle states are being produced. Thus, we will now move on to a discussion of searches for these new particle states.

SEARCH FOR NONLEPTONIC DECAYS OF CHARMED PARTICLES

We have searched for nonleptonic decays of charmed mesons by looking for narrow peaks in inclusive two and three body state invariant mass distributions in various modes.[11] The data sample was about 10,000 hadronic events at c.m. energy 4.8 GeV. This was the largest data sample available until quite recently.

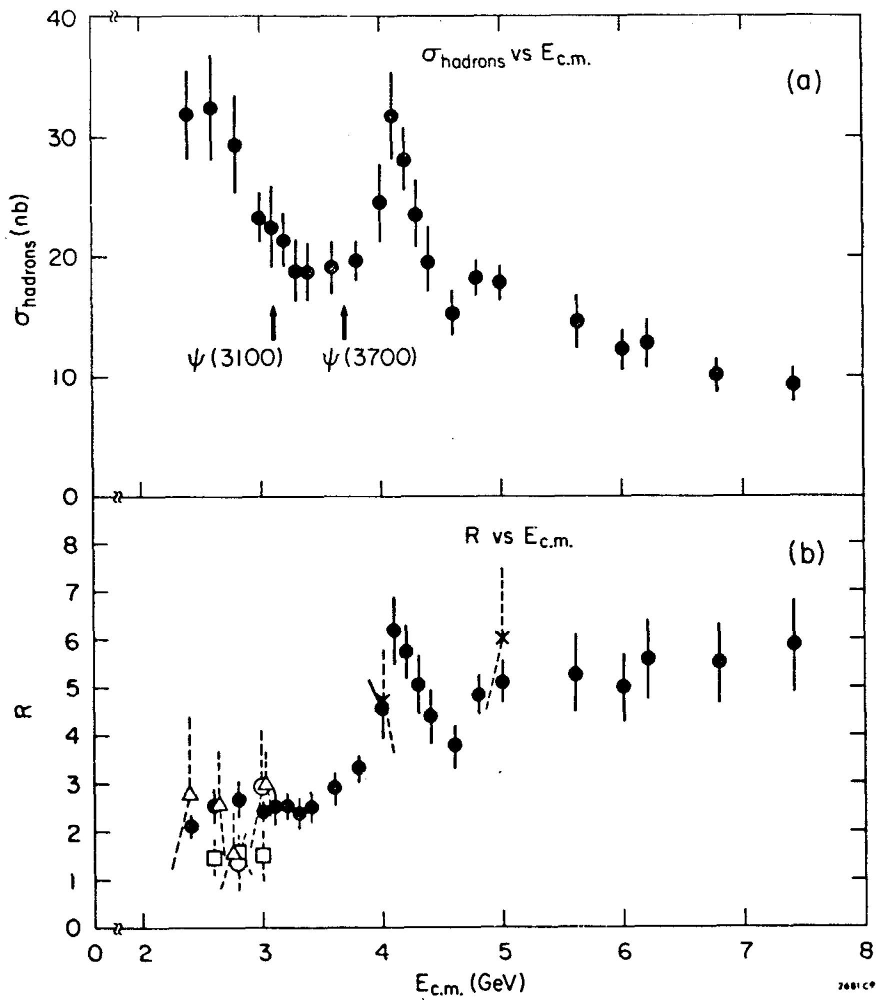

Fig. 19--(a) The total hadronic cross section versus center-of-mass energy.
(b) The ratio R of the total hadronic cross section to the theoretical muon pair production cross section. The dotted points are older results from Frascati and the CEA.

Data for a typical mode are shown in Fig. 20. This plot shows one of the two four standard deviation peaks which were observed - the bump at 2.40 GeV/c^2. (The other was at 2.05 GeV/c^2 in the $K_S^0K^{\pm}$ mode.) We do not consider either of these peaks significant since they could not be found in the 5.0 GeV data sample.

Upper limits have been set for eight modes and they are listed in Table V. These limits are a factor of two to five higher than what would be expected from conventional models.[12] However, the limits are probably not stringent enough to rule out the charm model.

EVIDENCE FOR ANOMALOUS LEPTON PRODUCTION

We have observed evidence for anomalous lepton production in the SLAC-LBL magnetic detector which cannot be explained by any conventional process.[13] The

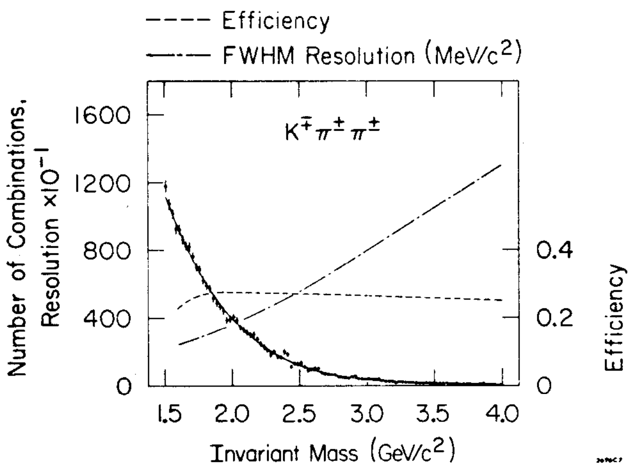

Fig. 20--Observed invariant mass distributions for $K^-\pi^+\pi^+$ and $K^+\pi^-\pi^-$ combinations. The solid line represents a smooth curve fitted to the data.

primary evidence is 24 events at $E_{c.m.} = 4.8$ GeV which appear to contain an electron and a muon, but no other visible charged or neutral particles. There are conventional processes which can yield events of this type through misidentifications, but calculations of these backgrounds give only 4 to 6 events. Various internal checks make it very unlikely that these events come from known processes.

TABLE V

Upper limits at the 90% confidence level for inclusive production cross section times branching ratio (nb)

Decay Mode	Mass Region (GeV/c^2) 1.50 to 1.85	1.85 to 2.40	2.40 to 4.00
$K^-\pi^+$ and $K^+\pi^-$	0.25	0.18	0.08
$K^0_s\pi^+\pi^-$	0.57	0.40	0.29
$\pi^+\pi^-$	0.13	0.13	0.09
K^+K^-	0.23	0.12	0.10
$K^-\pi^+\pi^+$ and $K^+\pi^-\pi^-$	0.51	0.49	0.19
$K^0_s\pi^+$ and $K^0_s\pi^-$	0.26	0.27	0.09
$K^0_sK^+$ and $K^0_sK^-$	0.54	0.33	0.09
$\pi^+\pi^-\pi^+$ and $\pi^+\pi^-\pi^-$	0.48	0.38	0.18
$K^\mp\pi^\pm$, $\bar{K}^0\pi^+\pi^-$ and $K^0\pi^+\pi^-$	1.16	0.90	0.58
K^+K^- and $\pi^+\pi^-$	0.23	0.16	0.15
$K^\mp\pi^\pm\pi^\pm$, $\bar{K}^0\pi^\pm$ and $K^0\pi^\pm$	0.64	0.51	0.30
$\bar{K}^0K^\pm$, $K^0K^\pm$ and $\pi^+\pi^-\pi^\pm$	1.10	0.76	0.29

Possible processes which could give events of this type are heavy lepton production,

$$
\begin{array}{l}
e^+e^- \rightarrow L^+L^- \\
\quad\quad\quad\; | \;\;\; \llcorner\!\!\rightarrow e^-\bar{\nu}_e \nu_L \\
\quad\quad\quad\; \llcorner\!\!\longrightarrow \mu^+ \nu_\mu \bar{\nu}_L
\end{array}
\tag{28}
$$

or production of a new heavy spin one boson which decays weakly,

$$
\begin{array}{l}
e^+e^- \rightarrow M^+M^- \\
\quad\quad\quad\; | \;\;\; \llcorner\!\!\rightarrow e^-\bar{\nu}_e \\
\quad\quad\quad\; \llcorner\!\!\longrightarrow \mu^+ \nu_\mu \; .
\end{array}
\tag{29}
$$

There are also other possibilities. We have not yet been able to determine which process is occurring.

Candidates for anomalous lepton production in the e^+e^- and $\mu^+\mu^-$ modes have also been observed.

The observed cross sections into the $e\mu$ mode at 4.8 GeV and several other energies are shown in Fig. 21. Corrections for geometrical and momentum cuts, which depend on the process and may be a factor of 2 to 10, have not been made.

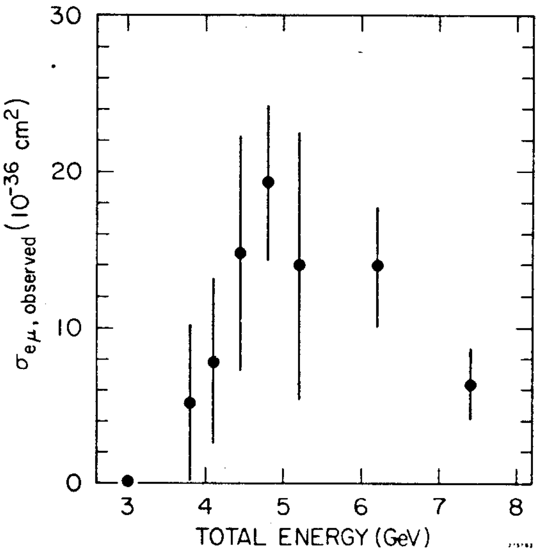

Fig. 21--The observed cross section for observing an e and a μ with no other particles in the SLAC-LBL magnetic detector. These data have not been corrected for momentum and angle cuts and for the geometry of the detector. This correction can be a factor of 2 to 10 depending on the origin of the events.

SUMMARY

We have observed two incredibly narrow resonances produced by e^+e^- annihilation and have

(a) measured their widths,

(b) determined their spin-parity to be $J^{PC} = 1^{--}$,

(c) determined that they couple to leptons via a photon,

(d) observed that isospin appears to be conserved in their decay and that both have $I^G = 0^-$,

(e) presented evidence that the ψ may be an SU(3) singlet,

(f) studied hadronic decays of the ψ,

(g) observed that the ψ' decays to the ψ a majority of the time, which implies that they are closely related, and

(h) noted that ψ' decays to ordinary hadrons have not been observed, which leaves about 40% of ψ' decays a mystery.

We have also measured the total hadronic cross section from 2.4 to 7.4 GeV and have observed two regions in which R is flat and a broad enhancement around 4.1 GeV. The step in R suggests the likelihood that new particle production is occurring beyond 4 GeV. The search for nonleptonic decays of new particles produced only upper limits, but there is evidence for new particle production in the form of anomalous lepton production.

POSTSCRIPT: ψ' RADIATIVE DECAYS

The editors of these Proceedings requested that I include a summary of post-conference work at SPEAR[14,15] on ψ' radiative decays to new states.

We have observed $\psi' \to \gamma\chi$, where χ is observed to decay into hadrons and/or $\gamma\psi$. The data require the existence of at least three χ states. (We use χ as a generic name for new C-even states radiatively coupled to the ψ particles.)

The decay $\chi \to 4\pi^{\pm}$ was found by observing that there is a clustering of events in ψ' decays with missing momentum between 100 and 300 MeV/c, whose missing mass is consistent with that of a γ, but not consistent with that of a π^0. (These events are visible in Fig. 18d.) After a 1-c fit, the χ mass spectrum in this mode exhibits a narrow peak at $3.41 \pm .01$ MeV/c^2 (~ 50 MeV/c^2 wide, consistent with our mass resolution) and a broader structure centered at $3.53 \pm .02$ MeV/c^2. The width of the latter state implies that either it is broad or, more likely, that it is composed of two or more unresolved narrow states.

There are eleven events which are consistent only with $\chi(3410) \to \pi^+\pi^-$ or $\chi(3410) \to K^+K^-$. These events require that the spin-parity of the $\chi(3410)$ be $J^{PC} = (\text{even})^{++}$. There are no observed events which are consistent with $\chi(3530) \to \pi^+\pi^-$ or K^+K^-.

There is also evidence for both the $\chi(3410)$ and $\chi(3530)$ decays to $6\pi^{\pm}$ and $\pi^+\pi^-K^+K^-$.

The decay $\chi \to \gamma\psi$ has been observed in two ways. The first method is to observe both γ's from $\psi' \to \gamma\gamma\psi$ in the shower counters and to detect the ψ by observing its decay into $\mu^+\mu^-$. Fifty-one events have been observed by this technique. The second method is to detect the $\mu^+\mu^-$ and only one photon; but the photon is detected by observing its conversion to an e^+e^- pair in the material around the beam pipe. Only six events have been observed by this method, but with good mass resolution (7 MeV/c^2 rms).

Data from both methods are consistent with the existence of a narrow state at either 3.50 ± 0.01 or 3.27 ± 0.01 GeV/c^2. The ambiguity exists since we cannot tell which photon was emitted first in the cascade decay.

It is tempting to identify the state which decays to $\gamma\psi$ with the χ (3530) which was observed in the $4\pi^{\pm}$ decay. However, due to the difference in widths as well as the difference in central mass values, this can be done only if the χ (3530) is composed of two or more unresolved states. Therefore, regardless of whether the higher or lower mass solution for the state which decays to $\gamma\psi$ is correct, there must be at least three χ states.

REFERENCES

1. The present members of the SLAC-LBL collaboration are: A. M. Boyarski, M. Breidenbach, F. Bulos, G. J. Feldman, D. Fryberger, G. Hanson, D. L. Hartill, B. Jean-Marie, R. R. Larsen, D. Lüke, V. Lüth, H. L. Lynch, C. C. Morehouse, J. M. Paterson, M. L. Perl, T. P. Pun, P. A. Rapidis, B. Richter, R. F. Schwitters, W. Tanenbaum, and F. Vannucci (Stanford Linear Accelerator Center); G. S. Abrams, W. Chinowsky, C. E. Friedberg, G. Goldhaber, J. A. Kadyk, A. M. Litke, B. A. Lulu, F. M. Pierre, B. Sadoulet, G. H. Trilling, J. S. Whitaker, F. Winkelmann, and J. E. Wiss (Lawrence Berkeley Laboratory).
2. For a more detailed description of the detector see J.-E. Augustin et al., Phys. Rev. Letters 34, 233 (1975), or G. J. Feldman and M. L. Perl, Phys. Reports 19C, 233 (1975), Appendix A.
3. A. M. Boyarski et al., Phys. Rev. Letters 34, 1357 (1975).
4. V. Lüth, A. M. Boyarski, H. L. Lynch et al., Stanford Linear Accelerator Center Report No. SLAC-PUB-1617 (1975).
5. D. R. Yennie, Phys. Rev. Letters 34, 239 (1975).
6. G. S. Abrams et al., Phys. Rev. Letters 34, 1181 (1975).
7. G. J. Feldman and F. J. Gilman, Stanford Linear Accelerator Center Report No. SLAC-PUB-1582 (1975).
8. T. Appelquist et al., Phys. Rev. Letters 34, 365 (1975); E. Eichten et al., Phys. Rev. Letters 34, 369 (1975).
9. J. W. Simpson et al., Stanford University Report No. HEPL 759 (1975).
10. J.-E. Augustin et al., Phys. Rev. Letters 34, 764 (1975).
11. A. M. Boyarski et al., Phys. Rev. Letters 35, 196 (1975).
12. M. K. Gaillard, B. W. Lee, and J. L. Rosner, Rev. Mod. Phys. 47, 277 (1975).
13. The oral version of this portion of the talk closely followed M. L. Perl, SLAC Report No. SLAC-PUB-1592 (1975), to be published in the proceedings of the Inst. of Particle Physics Summer School, McGill University, June 16-21, 1975. The reader is referred to this report for details.

14. G. J. Feldman, B. Jean-Marie, B. Sadoulet, F. Vannucci et al., SLAC Report No. SLAC-PUB-1621 (1975), and W. Tanenbaum, J. S. Whitaker et al., SLAC Report No. SLAC-PUB-1644 (1975).

15. Evidence for new states has also been found at DESY. See W. Braunschweig et al., DESY Report No. 75/20 (1975); B. Wiik and J. Heintze, invited talks at the 1975 Int. Symposium on Lepton and Photon Interactions at High Energies, Stanford University, August 21-27, 1975.